

# Search for Interstellar Adenine

Sandip K. Chakrabarti

*S. N. Bose National Centre for Basic Sciences, Salt Lake, Kolkata- 700098, India*

*§*

*Indian Centre for Space Physics, Chalantika 43, Garia Station Road, Kolkata- 700084, India*

Liton Majumdar

*Indian Centre for Space Physics, Chalantika 43, Garia Station Road, Kolkata- 700084, India*

Ankan Das

*Indian Centre for Space Physics, Chalantika 43, Garia Station Road, Kolkata- 700084, India*

Sonali Chakrabarti

*Maharaja Manindra Chandra College, 20 Ramakanto Bose Street, Kolkata- 700003, India*

*§*

*Indian Centre for Space Physics, Chalantika 43, Garia Station Road, Kolkata- 700084, India*

## ABSTRACT

It is long debated if pre-biotic molecules are indeed present in the interstellar medium. Despite substantial works pointing to their existence, pre-biotic molecules are yet to be discovered with a complete confidence. In this paper, our main aim is to study the chemical evolution of interstellar adenine under various circumstances. We prepare a large gas-grain chemical network by considering various pathways for the formation of adenine. Majumdar et al. (2012) proposed that in the absence of adenine detection, one could try to trace two precursors of adenine, namely, HCCN and NH<sub>2</sub>CN. Recently Merz et al. (2014), proposed another route for the formation of adenine in interstellar condition. They proposed two more precursor molecules. But it was not verified by any accurate gas-grain chemical model. Neither was it known if the production rate would be high or low. Our paper fills this important gap. We include this new pathways to find that the contribution through this pathways for the formation of Adenine is the most dominant one in the context of interstellar medium. We propose that observers may look for the two precursors (C<sub>3</sub>NH and HNCNH) in the interstellar media which are equally important for predicting abundances of adenine. We perform quantum chemical calculations to find out spectral properties of adenine and its two new precursor molecules in infrared, ultraviolet and sub-millimeter region. Our present study would be useful for predicting abundance of adenine.

*Subject headings:* Bio-molecules, Interstellar Medium, Astrochemistry, Molecular cloud, Star formation

## 1. Introduction

According to the Cologne Database for Molecular Spectroscopy (Muller et al. 2001, 2005), around 180 molecules have been detected in the in-

terstellar medium (ISM) or in circumstellar shells. Among these, several species are organic in nature. Existence of these complex molecules could not be explained without a proper consideration of interstellar dusts (Hasegawa, Herbst & Leung

1992; Das, Acharyya & Chakrabarti 2010; Boogert & Ehrenfreund 2004; Gibb et al. 2004). Several attempts were made over the past few years to study physical and chemical processes on the interstellar grains (Chakrabarti et al. 2000a,b; Cuppen & Herbst 2007; Das et al. 2008b; Das, Acharyya & Chakrabarti 2010; Das et al. 2013b; sahu 2015). Several experimental results have been reported in explaining the importance of various surface processes on interstellar dusts (Ioppolo et al. 2008; Oberg et al. 2009), making it imperative to incorporate the grain surface chemistry extensively while predicting their abundances.

The problem of Origin of life is a long standing puzzle and formation of amino acids in the laboratory by well known work of Miller (1953) ushered a new direction of research in this area. More recently, Chakrabarti & Chakrabarti (2000a,b) for the first time, suggested that perhaps the process of formation of the complex molecules such as Adenine and other constituents of DNA is very generic and such complex pre-biotic molecules should be formed during any star forming process. In the absence of proper reaction cross sections, Chakrabarti & Chakrabarti (2000a) used neutral-neutral reaction rates to compute adenine abundance with successive addition of HCN. This was later improved upon with more realistic cross sections (Chakrabarti & Chakrabarti 2000b) and more realistic abundance was obtained. Presence of interstellar grains were in explicitly added in these works, and were incorporated indirectly by a higher rate coefficients in  $H_2$  formation. A follow up study by Majumdar et al. (2012) explicitly considered presence of grains and showed that this significantly alters the abundance of adenine. They carried out several prescriptions of rate coefficients for successive HCN addition reactions. They also considered radical-radical/radical-molecular reactions proposed by Gupta et al. (2011) for the formation of adenine. Their results suggest that radical-radical/ radical-molecular reactions dominates over the neutral-neutral reactions. Recently Merz et al. (2014) used the concept of retro-synthetic analysis to produce interstellar adenine from observed interstellar molecules such as  $C_3NH$ ,  $HNCNH$  and its isomer  $H_2NCN$ . They used MP2/6-311++G(2d,2p) method to calculate various chemical parameters involving a six step mechanism. This motivated us

to perform a comparative study among various available pathways for the formation of adenine in interstellar region. This we present below.

The plan of this paper is the following. In Section 2, computational methods are discussed. Results are presented in Section 3, and finally in Section 4, we draw our conclusions.

## 2. Methods and Computational Details

### 2.1. Chemical modeling

We develop a large gas-grain chemical network to explore chemical evolution of interstellar adenine and its related species. For the gas-phase chemical network, we follow UMIST 2006 data base. Formation of adenine via various reaction pathways used in Chakrabarti & Chakrabarti (2000a,b), Gupta et al. (2011) and Merz et al. (2014) are included. Our gas phase chemical network consists of more than 6000 reactions between 650 species.

For the grain surface reaction network, we follow Hasegawa, Herbst & Leung (1992); Cuppen & Herbst (2007); Das, Acharyya & Chakrabarti (2010); Das & Chakrabarti (2011); Das et al. (2013b, 2015). Our surface reaction network contains 292 reactions. We consider gas-grain interaction to frame the actual interstellar scenario. Gas phase species are allowed to accrete on interstellar grains. Grains are actually acting as a catalyst for the formation of several complex interstellar species. Formation of the simple and most abundant interstellar molecule,  $H_2$  cannot not be explained without the consideration of interstellar grain chemistry. Binding energies of surface species mainly dictate chemical composition of interstellar grain mantle. We consider the most updated interaction barrier energies as mentioned in Das et al. (2013b) and references therein. Depending on the energy barriers, surface species would move throughout the grain surface by thermal hopping or tunneling whichever is faster. At low temperatures, for lighter species such as H atom, tunneling is much faster. During these movements, surface species would react with any suitable reactant partners. Based on their energy barriers, surface species would also thermally evaporate (Hasegawa, Herbst & Leung 1992) and populate the gas phase. Cosmic ray induced evaporation (hasegawa & Herbst 1993) and non-thermal desorption (Garrod, Wakelam & Herbst

Table 1: Available and estimated rate co-efficients for the formation of interstellar adenine in the gas phase via various reaction pathways

Pathways used in	Reactions	Rate coefficients
Chakrabarti & Chakrabarti (2000a,b), Majumdar et al. (2012)	(i) $\text{HCN} + \text{HCN} \rightarrow \text{CH}(\text{NH})\text{CN}$	$8.38 \times 10^{-20} \text{ cm}^3 \text{ sec}^{-1}$
	(ii) $\text{CH}(\text{NH})\text{CN} + \text{HCN} \rightarrow \text{NH}_2\text{CH}(\text{CN})_2$	$3.43 \times 10^{-12} \text{ cm}^3 \text{ sec}^{-1}$
	(iii) $\text{NH}_2\text{CH}(\text{CN})_2 + \text{HCN} \rightarrow \text{NH}_2(\text{CN})\text{C} = \text{C}(\text{CN})\text{NH}_2$	$3.30 \times 10^{-15} \text{ cm}^3 \text{ sec}^{-1}$
	(iv) $\text{NH}_2(\text{CN})\text{C} = \text{C}(\text{CN})\text{NH}_2 + \text{HCN} \rightarrow \text{C}_5\text{H}_5\text{N}_5$	$3.99 \times 10^{-10} \text{ cm}^3 \text{ sec}^{-1}$
Gupta et al. (2011)	(v) $\text{HCCN} + \text{HCN} \rightarrow \text{Molecule 1}$	$2.13 \times 10^{-17} \text{ cm}^3 \text{ sec}^{-1}$
	(vi) $\text{Molecule 1} + \text{H} \rightarrow \text{Molecule 2}$	$7.96 \times 10^{-9} \text{ cm}^3 \text{ sec}^{-1}$
	(vii) $\text{Molecule 2} + \text{NH}_2\text{CN} \rightarrow \text{Molecule 3}$	$6.24 \times 10^{-12} \text{ cm}^3 \text{ sec}^{-1}$
	(viii) $\text{Molecule 3} + \text{CN} \rightarrow \text{Molecule 4}$	$1.80 \times 10^{-9} \text{ cm}^3 \text{ sec}^{-1}$
	(ix) $\text{Molecule 4} + \text{H} \rightarrow \text{Molecule 5}$	$8.71 \times 10^{-9} \text{ cm}^3 \text{ sec}^{-1}$
	(x) $\text{Molecule 5} + \text{CN} \rightarrow \text{C}_5\text{H}_5\text{N}_5 + \text{HNC}$	$1.89 \times 10^{-9} \text{ cm}^3 \text{ sec}^{-1}$
	(xi) $\text{Molecule 5} + \text{CN} \rightarrow \text{C}_5\text{H}_5\text{N}_5 + \text{HCN}$	$1.91 \times 10^{-9} \text{ cm}^3 \text{ sec}^{-1}$
Merz et al. (2014)	(xii) $\text{C}_3\text{NH} + \text{HNCNH} \rightarrow \text{C}_4\text{N}_3\text{H}_3$	$8.30 \times 10^{-20} \text{ cm}^3 \text{ sec}^{-1}$
	(xiii) $\text{C}_4\text{N}_3\text{H}_3 + \text{HNCNH} \rightarrow \text{C}_4\text{H}_3\text{N}_3 + \text{NH}_2\text{CN}$	$6.43 \times 10^{-22} \text{ cm}^3 \text{ sec}^{-1}$
	(xiv) $\text{C}_4\text{H}_3\text{N}_3 + \text{HNCNH} \rightarrow \text{C}_5\text{N}_5\text{H}_5$	$1.36 \times 10^{-9} \text{ sec}^{-1}$
	(xv) $\text{C}_5\text{N}_5\text{H}_5 + \text{HNCNH} \rightarrow \text{N}_5\text{C}_5\text{H}_5 + \text{NH}_2\text{CN}$	$1.00 \times 10^{-9} \text{ cm}^3 \text{ sec}^{-1}$
	(xvi) $\text{N}_5\text{C}_5\text{H}_5 + \text{HNCNH} \rightarrow \text{C}_5\text{H}_5\text{N}_5 + \text{NH}_2\text{CN}$	$1.89 \times 10^{-13} \text{ sec}^{-1}$

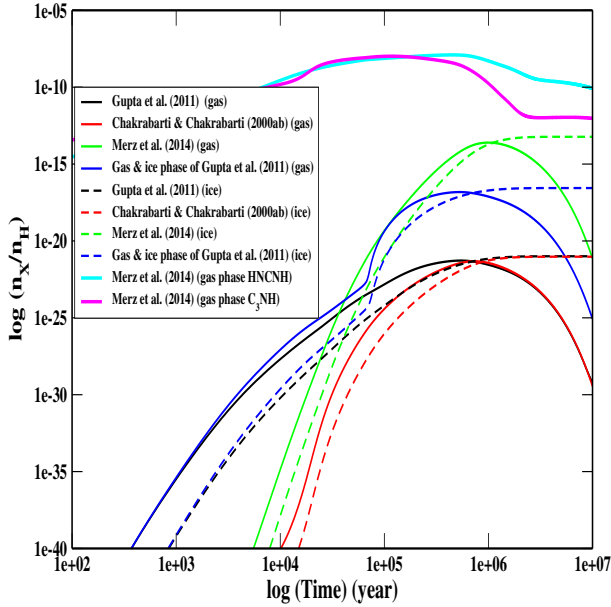


Fig. 1.— Comparison of results of various adenine formation pathways. Pathways proposed by Merz et al. (2014) is dominating over all other pathways.

2007; Das et al. 2015) mechanisms are also considered in our model. So, in brief, gas and grains are interacting with each other to exchange their chemical components by various means. Since all the processes are random, Monte Carlo method would be appropriate to use while dealing with this randomness. However, it requires huge computational time to compute with our vast gas phase and grain phase chemical networks simultaneously. Thus, we use traditional Rate equation method to handle our chemical network on grains. Detailed discussions on our gas-grain chemical model are already presented in Das et al. (2013b, 2015); Majumdar, Das & Chakrabarti (2014a,b).

All the reactions, which are considered here for the formation of adenine are shown in Table 1. Majumdar et al. (2012, 2013) considered neutral-neutral pathways (reaction number (i)-(iv) of Table 1) of Chakrabarti & Chakrabarti (2000a,b) and radical-radical/radical-molecular pathways (reaction numbers (v)-(xi)) of Gupta et al. (2011) and concluded that the production of adenine is dominated by radical-radical/radical-molecular reaction pathways. They identified HCCN and  $\text{NH}_2\text{CN}$  as two main precursor molecules, which are responsible for the production of adenine. HCCN is highly abundant in the interstellar space (Jiurys 2006; Guelin & Cernicharo 1991). Formation of HCCN on the interstellar grains were also considered (Hasegawa, Herbst & Leung 1992). McGonagale & Irvine (1996) conducted a deep search for HCCN towards TMC-1 and several GMC's via its  $N(J) = 1(2) \rightarrow 0(1)$  transition.

They came up with an upper limit of fractional abundance with respect to molecular hydrogen to be  $\sim 2 \times 10^{-10}$ . Existence of  $\text{NH}_2\text{CN}$  in the interstellar cloud was first reported by Turner et al. (1975). Subsequently, it was observed in both diffuse and dense clouds by Liszt & Lucas (2001). Woodall et al. (2007) predicted a steady state fractional abundance of  $2.02 \times 10^{-10}$  for  $\text{NH}_2\text{CN}$  with respect to  $\text{H}_2$ .

Merz et al. (2014) proposed a new pathway (reaction nos. x(ii)-(xvi) of Table 1) for the production of adenine. They used retro synthetic analysis by using two new species ( $\text{C}_3\text{NH}$  and  $\text{HNCNH}$ ). Carbodimide ( $\text{HNCNH}$ ), is an isomer of cyanamide ( $\text{NH}_2\text{CN}$ ). McGuire et al. (2013) obtained the abundance of this molecule from ice mantle experiments. They proposed that tautomerization of  $\text{NH}_2\text{CN}$  on dust grain ice mantles is the dominant formation pathway for  $\text{HNCNH}$ . They found its abundance would be  $\sim 10\%$  of  $\text{NH}_2\text{CN}$  (in Sgr B2(N) column density of  $\text{NH}_2\text{CN}$  is  $\sim 2 \times 10^{13} \text{ cm}^{-2}$ ). Since, this was below the detection limit of any current astronomical facility, they proposed to observe  $\text{HNCNH}$  by those transitions which are amplified by masing. In our chemical model, we consider that 10% of  $\text{NH}_2\text{CN}$  could be converted into  $\text{HNCNH}$ .

We use semi-empirical relationship developed by Bates (1983) for the computation of rate coefficients of the exothermic and barrier less reaction pathways (reaction nos. xii-xiv) of Merz et al. (2014).

$$K = 1 \times 10^{-21} A_r (6E_0 + N - 2)^{(3N-7)} / (3N-7)! \text{ cm}^3 \text{ s}^{-1} \quad (1)$$

where,  $E_0$  is the association energy in eV,  $A_r$  is the transition probability (in  $\text{s}^{-1}$ ) of the stabilizing transition (the numerical value of which may be taken to be 100 unless better information is available) and  $N$  is the number of nuclei in reactants. For the reaction numbers xii, xiii & xiv, we use association energies of  $-5.2$ ,  $-0.6$ ,  $-72.8$  kcal/mol respectively.

If the calculated rate coefficients from Eqn. 1 exceeds the limit set by the following equation (Eqn. 2), then this limiting value was adopted:

$$K = 7.41 \times 10^{-10} \alpha^{1/2} (10/\mu)^{1/2} \text{ cm}^3 \text{ s}^{-1} \quad (2)$$

where,  $\alpha$  is the polarizability in  $\text{\AA}^3$ ,  $\mu$  is the reduced mass of the reactants in  $^{12}\text{C}$  amu scale as

suggested by Bates (1983).

Rate coefficients of reactions having activation barriers (reaction nos. xv-xvi) are calculated by using conventional transition state theory. According to this theory, the rate coefficient has the following form:

$$k(T) = (K_B T / h C_0) \exp(-\Delta G / RT) \text{ s}^{-1}, \quad (3)$$

where,  $K_B$  is the Boltzmann constant,  $h$  is the Plank's constant,  $T$  is the temperature,  $C_0$  is the concentration (set to 1, by following Jalbout et al. (2008)),  $R$  is the ideal gas constant, and  $\Delta G$  is the free energy of activation. From the quantum chemical calculations by Merz et al. (2014), we are having  $\Delta G = +0.4$  kcal/mol and  $+1.1$  kcal/mol respectively for reaction numbers xv and xvi.

## 2.2. Spectroscopic Modeling

An educated estimate of spectral properties is essential before observing any unidentified species. It is reported in earlier astrophysical literature that DFT and TDDFT (Runge & Gross 1984) computation methods would be applied to various astrophysical problems (Puletti et al. 2010; Pieve et al. 2014). Das et al. (2015) discussed the necessity of quantum chemical calculations prior to any spectroscopical survey. Since our chemical model would predict the abundances of adenine and its related species, we believe it would be useful to present various spectral aspects of these species. For finding the various spectral aspects, we perform quantum chemical calculations by using Gaussian 09W program. By following Majumdar, Das & Chakrabarti (2014b), for the vibrational frequencies, we use B3LYP/6-311++G(d,p) level of theory. In case of grain phase species, Polarizable Continuum Model (PCM) is used with the integral equation formalism variant (IEFPCM) as the default SCRF method. For the electronic absorption spectrum, we use time dependent density functional theory (TDDFT study). Since most of the gas phase complex molecules were observed by their rotational transitions in the mm or sub-mm regime, we carry out quantum chemical calculations to find out the rotational transitions of our desired species. Computation of the anharmonic frequencies require the use of analytic second derivative of energies at the displaced geometries. But the CCSD method in Gaussian 09W program only implements energies,

Table 2: Initial elemental abundances

Species	Abundance
H <sub>2</sub>	$5.00 \times 10^{-01}$
He	$1.00 \times 10^{-01}$
N	$2.14 \times 10^{-05}$
O	$1.76 \times 10^{-04}$
H <sub>3</sub> <sup>+</sup>	$1.00 \times 10^{-11}$
C <sup>+</sup>	$7.30 \times 10^{-05}$
S <sup>+</sup>	$8.00 \times 10^{-08}$
Si <sup>+</sup>	$8.00 \times 10^{-09}$
Fe <sup>+</sup>	$3.00 \times 10^{-09}$
Na <sup>+</sup>	$2.00 \times 10^{-09}$
Mg <sup>+</sup>	$7.00 \times 10^{-09}$
P <sup>+</sup>	$3.00 \times 10^{-09}$
Cl <sup>+</sup>	$4.00 \times 10^{-09}$
e <sup>-</sup>	$7.31 \times 10^{-05}$
HD	$1.6 \times 10^{-05}$

so analytic second derivative of energies are not available at this level of theory. So there are no options in Gaussian 09W program to compute the rotational and distortional constants at the CCSD level of theory. Here, we use B3LYP/aug-cc-pvTZ level of theory, which are also proven to be very accurate (Carles et al. 2013; Das et al. 2015). This level of theory would be appropriate because there are some earlier studies (such as, Brunken et al. (2006)) for finding rotational and distortional constants of Uracil (one nucleo base of RNA beside adenine, cytosine and guanine). Corrections for the interaction between the rotational motion and vibrational motion along with the corrections for vibrational averaging and an-harmonic corrections to the vibrational motion are also considered in our calculations. Obtained rotational and distortional constants are then used in SPCAT (Pickett 1991) program to predict various rotational transitions. Output of the SPCAT program is then directly used in ASCP Prgram (Kisiel et al. 1998, 2000) to find out the rotational stick diagram of the desired species.

### 3. Results and Discussion

#### 3.1. Results of Chemical modeling

Chakrabarti & Chakrabarti (2000a,b); Majumda (2012) considered successive HCN addition for the formation of adenine. Gupta et al. (2011) proposed adenine formation pathways starting with HCCN and HCN. Gupta et al. (2011) also pointed out that their reaction pathways would also be feasible in the grain phase. A completely new pathway has been proposed recently

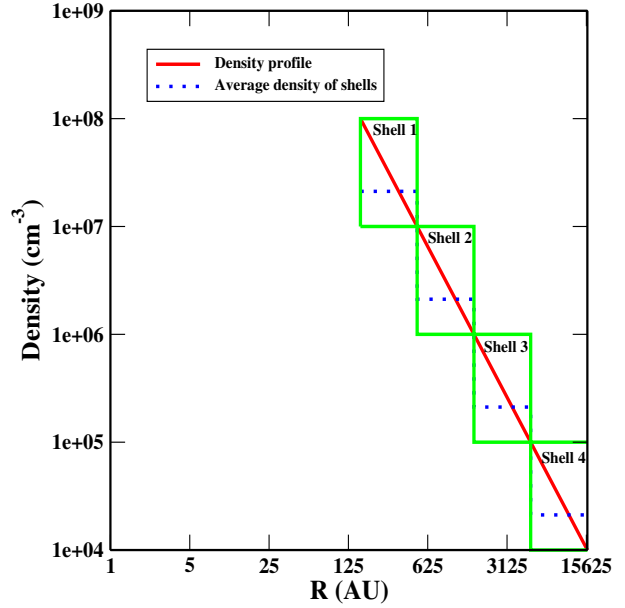


Fig. 2.— Radial distribution of density profile.

by Merz et al. (2014), where adenine could be produced without any HCN addition. So, we wish to compare four different pathways where the first one is the gas phase pathway of Gupta et al. (2011), the second one is the pathway considered by Chakrabarti & Chakrabarti (2000a,b) and updated by Majumdar et al. (2012), the third one is the gas phase pathway proposed by Merz et al. (2014). As a fourth method, we consider both gas and grain phase pathways of Gupta et al. (2011). Since, no mention was made of the grain phase reactions in Merz et al. (2014) and Chakrabarti & Chakrabarti (2000a,b), we do not consider these pathways in the grain phase. In general, we consider that the gas and the grain interact with each other to exchange their chemical components. So, grain phase could be populated by the accretion from the gas phase and gas phase could be populated by the grain phase species through evaporation mechanisms such as, thermal desorption, non-thermal desorption and cosmic-ray induced desorption. Initial elemental abundances with respect to total hydrogen nuclei (Table 2) are considered to be similar to what is in Das et al. (2013b) and Majumdar, Das & Chakrabarti (2014b). These are the typical low metallic abundances which are often adopted for TMC-1 cloud. In Fig. 1, a comparative study between these four pathways are shown for the chemical evolution of adenine. To draw this, we take number density of hydrogen nuclei existing in all possible forms ( $n_H$ ) to be  $= 10^4 \text{ cm}^{-3}$ ,  $A_V = 10$  and  $T = 10 \text{ K}$ . Various evaporation mechanisms are considered here, among them, around low temperatures, non-thermal desorption mechanism (Garrod, Wakelam & Herbst 2007; Das et al. 2015) is the most efficient means to transfer these complex molecules to the gas phase. A moderate value of the desorption parameter ( $\sim 0.05$ ) is considered. Significant difference in the abundance of adenine could be observed between the two considerations of Gupta et al. (2011). In one case, only gas phase pathways of Gupta et al. (2011) is considered and in another case, the same pathways are considered for both the phases (gas and grain). From Fig. 1, we find that the peak abundances of adenine for these two cases appear to be  $5.3 \times 10^{-22}$  and  $1.5 \times 10^{-17}$  respectively. Since grain phase production is efficient, produc-

tion is significantly enhanced in the case when grain phase pathways are also considered. While using pathways of Chakrabarti & Chakrabarti (2000a,b), peak abundance of adenine turns out to be  $4.8 \times 10^{-22}$  and using pathways proposed by Merz et al. (2014), the peak abundance becomes  $2.5 \times 10^{-14}$ . Using neutral-neutral rate coefficients in an isothermal cloud, Chakrabarti & Chakrabarti (2000a) found the abundance of  $\sim 5 \times 10^{-13}$ , one magnitude higher than this. It is also clear from Fig. 1 that the adenine formation pathways of Merz et al. (2014) dominates over all other pathways. In Fig. 1, we show chemical evolutions of HNCNH and  $C_3NH$  (which are required for the formation of adenine in the pathways proposed by Merz et al. (2014)). These molecules could be used as the precursors for estimating the abundances of adenine in interstellar region.

### 3.1.1. Mixing model

Chemical complexity of any interstellar region is highly dependent on surrounding physical condition. Formation of bio-molecules would also be influenced by surrounding physical process. To describe a realistic situation, we prepare a special model named “Mixing model”. We consider that density profile follows  $\rho \sim r^{-2}$  distribution as described by Shu (1977). At the outer boundary of the cloud the density is  $10^4 \text{ cm}^{-3}$ , inner boundary location is chosen in such way that the density would become  $10^8 \text{ cm}^{-3}$  (Fig. 2). For concreteness, we choose the outer boundary to be at 15962 AU and the inner boundary becomes at 159.62 AU. To reduce computational time we further subdivide this cloud into four shells, innermost shell is extended from 159.62 AU to 504.76 AU which has an average density of  $2.12 \times 10^7 \text{ cm}^{-3}$ . The shell no. 2 has an average density of  $2.12 \times 10^6 \text{ cm}^{-3}$  and extends from 504.76 AU to 1596.2 AU. The shell no. 3 has an average density of  $2.12 \times 10^5 \text{ cm}^{-3}$  and extends from 1596.2 AU to 5047.63 AU. The fourth shell extends from 5047.63 AU to 15962 AU and has an average density of  $2.12 \times 10^4 \text{ cm}^{-3}$ . Since the cloud is dense, we assume visual extinction ( $A_V$ ) of 10 and temperature 10 K throughout the cloud.

We assume that a systematic mixing is going on throughout the cloud. Matter of shell 4 would contribute ( $p_4\%$  of shell 4 matter) to shell 3, ma-

terial of shell 3 would contribute ( $p_3\%$  of shell 3 matter) to shell 2, material of shell 2 would contribute ( $p_2\%$  of shell 2 matter) to shell 1 and due to re-entry of the outflow at the outer edge, some matter would re-enter ( $p_1\%$  of shell 1 matter) into shell 4. Each transport should have different time scales. Inward material transfer (from shell 4  $\rightarrow$  shell 3  $\rightarrow$  shell 2  $\rightarrow$  shell 1) is assumed to take place with the sound speed of ( $\sqrt{\gamma KT/m_p} \sim 2.873 \times 10^4$  cm/s for  $T = 10$  K and  $\gamma = 5/3$ ). Since shell 4 is  $10914 AU$  thick, sound wave will take  $5.68 \times 10^{12}$  s ( $t_4$ ) to cross it. We assume that after every  $t_4$  second, some percentage matter would move to shell 3. Similarly, we calculate the time scale for transferring some fraction of matter from shell 3 to shell 2 ( $t_3 = 1.80 \times 10^{12}$  s) and shell 2 to shell 1 ( $t_2 = 5.68 \times 10^{11}$  s). Due to outflow, some fraction of matter of shell 1 would contribute to shell 4. Time scale for the outflow ( $t_1$ ) is chosen by considering free fall time scale ( $\sqrt{3\pi/32G\rho}$ ). Free fall time scale is inversely proportional to the square root of density. Here, we choose a typical dense cloud number density ( $10^4 \text{ cm}^{-3}$ ) for the calculation of free fall time. So in our case we assume  $t_1 = 1.62 \times 10^{13}$  s. For simplicity, we assume that  $p_4 = p_3 = p_2 = p_1 = 20\%$ .

In Fig. 3, depth dependence of peak and final adenine abundances are shown for the non-mixing and mixing cases with a density profile of Fig. 2. Abundances are represented with respect to the total hydrogen nuclei in all forms. For each shell, We carry out our simulation up to  $2 \times 10^6$  year. By the peak abundance, we mean the peak value obtained during the simulation regime and by the final abundance, we mean the value obtained at the end of simulation time scale. Since from Fig. 1, it is clear that the pathways of Merz et al. (2014) is dominating over all other existing pathways for the production of adenine in interstellar region, here, for Fig. 3, we considered only the pathways of Merz et al. (2014). Clearly, due to the mixing of matter among various shells, final abundance of adenine is severely affected in the mixing model. Peak abundances of adenine is decreasing inside the cloud. Reason behind is that as we penetrate inside the cloud, density increases and this results in shorter depletion (to the next shell) time scale. Due to heavy depletion, all related species depleted from the gas phase. As a result, the peak value of adenine is reduced. However,

the final value goes up and indeed, the final and the peak values become similar due to significant mixing.

## 3.2. Results of Spectroscopic modeling

### 3.2.1. Vibrational transitions

HNCNH is one of the isomers of  $\text{NH}_2\text{CN}$  which is a planar pentatonic molecule. It has nine fundamental vibrations (Rubalcava 1956). Similar to  $\text{NH}_2\text{CN}$ , HNCNH also has nine fundamental vibration lines as shown in Table 3. In Fig. 4a-c, infrared absorption spectra of HNCNH for the gas phase and grain phase are shown. We note that the gas phase HNCNH has its strongest feature at  $2225.48 \text{ cm}^{-1}$  and the second intense peak arises at  $899.71 \text{ cm}^{-1}$ . In the grain phase  $2225.48 \text{ cm}^{-1}$  peak is shifted to  $2179.37 \text{ cm}^{-1}$  and peak at  $899.71 \text{ cm}^{-1}$  is also shifted to  $925.14 \text{ cm}^{-1}$  with much lower intensity. Beside these intense peaks, there are several peaks which are pronounced in our grain phase model (such as peaks at  $902.61 \text{ cm}^{-1}$  and  $3564.13 \text{ cm}^{-1}$ ). For the sake of better understanding, we placed all the infrared peak positions with their absorbance in Table 3. Moreover, a comparison with the other theoretical/experimental vibrational transitions for HNCNH (Birk & Winnewisser, 1986; King & Strope, 1971) are also shown in Table 3. Some of our peak positions are very close to the results reported in the literature.

In Table 3, we also note down the peak position of the infrared spectrum of  $\text{C}_3\text{NH}$  in the gas as well as in the grain phase. We find that the most intense mode in the gas phase appears at  $2293.10 \text{ cm}^{-1}$ . This peak is shifted in the left side in the grain phase and appears at  $2309.68 \text{ cm}^{-1}$ . Among the other peaks in the gas phase,  $3718.05 \text{ cm}^{-1}$  and  $463.33 \text{ cm}^{-1}$  has the major contributions. One strong peak at  $3760.19 \text{ cm}^{-1}$  appears in the grain phase. Fig. 4c shows infrared spectra of adenine in gas and grain phases. Gas phase infrared spectrum of adenine contains strong peaks at  $1634.40 \text{ cm}^{-1}$ ,  $1656.77 \text{ cm}^{-1}$ ,  $31.23 \text{ cm}^{-1}$  and all these peaks are shifted to grain phase and appears at  $1638.84 \text{ cm}^{-1}$ ,  $1621.56 \text{ cm}^{-1}$ ,  $141.19 \text{ cm}^{-1}$ . Not only that, few new strong peaks appears at  $3594.23 \text{ cm}^{-1}$ ,  $3634 \text{ cm}^{-1}$ ,  $3718.16 \text{ cm}^{-1}$  for grain phase adenine. These features are clear in the Fig. 4c.

### 3.2.2. Electronic transitions

We continue our computation to obtain the spectral properties of  $C_3NH$  and  $HNCNH$  in the electronic absorption mode. Electronic absorption spectra of  $HNCNH$ ,  $C_3NH$  and adenine in gas as well in the grain phase are shown in Fig. 5a-c. Corresponding electronic transitions, absorbance and oscillator strengths are also summarized in Table 4. An electronic absorption spectrum of  $HNCNH$  molecule in the gas phase is characterized by five intense peaks. These five transitions occurred at 219.55, 184.83, 156.97, 141.48, 102 nm with major contributions from  $1-A1 \rightarrow 1-B2$ ,  $1-A1 \rightarrow 1-B1$ ,  $1-A1 \rightarrow 1-B2$ ,  $1-A1 \rightarrow 1-B2$  and  $1-A1 \rightarrow 1-A2$  electronic transitions. All the peaks are shifted in grain phase with the corresponding change in electronic transitions, absorbance and oscillator strength. For  $C_3NH$  molecule, electronic absorption spectra in gas as well in the grain phases are shown in Fig. 5b. This electronic spectrum in gas phase contains peaks at 182.6, 126.7, 104.04 nm due to  $1-A' \rightarrow 1-A'$ ,  $1-A' \rightarrow 1-A''$ ,  $1-A' \rightarrow 1-A'$ . As in case of  $HNCNH$ , here also corresponding gas phase peaks shift in the grain phase. However, most interestingly, the gas phase as well as grain phase adenine contains only one strong peak in the electronic mode shown in the Fig. 5c. Gas phase strong peak appears at 256.12 nm with oscillator strength 0.0655 for  $1-A \rightarrow 1-A$  electronic transition. This peak is shifted to grain phase and appears at 252.11 nm with oscillator strength 0.1267 for the same electronic transition.

### 3.2.3. Rotational transitions

In Table 5, we summarize our calculated rotational and distortional constants of the precursors  $HNCNH$  and  $C_3NH$  of adenine and adenine itself, in gas phase. Calculated constants are corrected for each vibrational state as well as vibrationally averaged structures. Here we use B3LYP/cc-pVTZ level to perform these calculations in gas phases. In Table 5, calculated distortional constants correspond to  $I^t$  representation with 'A' reduction. Figure 6 shows the stick diagram of two new precursors of adenine.

## 4. Concluding Remarks

Interstellar chemistry to form complex biomolecules began in this century and the first quantitative computation of adenine and other prebiotic molecules was presented by Chakrabarti & Chakrabarti (2000a,b). A follow up study by Majumdar et al. (2012) showed that formation of adenine mainly follows radical-radical/radical-molecular reaction pathways as proposed by Gupta et al. (2011). More recently, Merz et al. (2014) performed retro synthetic analysis to find out a new mechanism for adenine formation in the gas-phase. They proposed that it could be formed from three already known interstellar molecules, namely,  $C_3NH$  and the isomers,  $HNCNH$  and  $H_2NCN$ . Uniqueness of this pathway is that it does not involve HCN, water or ammonia during the production of adenine by any of the six intermediate steps. In this paper, we carried out a comparative study among various formation pathways of adenine. We considered all the pathways used in Chakrabarti & Chakrabarti (2000a,b); Gupta et al. (2011); Merz et al. (2014). Our chemical model suggests that the adenine formation pathways proposed by Merz et al. (2014) dominates over all other existing pathways. We studied the effects of mixing caused by both advection and outflows. We find that for adenine, though the peak abundance is severely reduced, the final abundance becomes higher as compared to the non-mixing (static evolution) case. We explored the infrared, electronic, sub-millimeter spectroscopy of adenine along with its two new precursor molecules ( $HNCNH$  and  $C_3NH$ ). We show that adenine will have one single strong line either in the gas or in the grain phase vibrational spectra. A detailed chemical and spectroscopical information about adenine as revealed by our analysis and its precursors would be extremely helpful for future survey of this species in the interstellar medium. In case the adenine is not directly detected, we believe that the detection of  $HNCNH$ ,  $H_2NCN$  and  $C_3NH$  would give adequate reason to believe that adenine must also be present.

## 5. Acknowledgments

AD, SKC are grateful to ISRO respond (Grant No. ISRO/RES/2/372/11-12) and DST (Grant No. SB/S2/HEP-021/2013) for financial support. LM thank MOES for funding during this work.



Table 3: Vibrational frequencies of precursors HNCNH and C<sub>3</sub>NH of adenine in gas phase and H<sub>2</sub>O ice containing grains at B3LYP/6-311G++(d,p) level

Species	Peak positions (Gas phase) (Wavenumber in $cm^{-1}$ )	Absorbance	Peak positions (water ice) (Wavenumber in $cm^{-1}$ )	Absorbance	Experiment or other theoretical value (Wavenumber in $cm^{-1}$ )
HNCNH	540.31	79.926	539.48	141.348	537 <sup>k</sup>
	540.65	0.195	539.60	0.142	
	718.17	107.962	719.18	140.079	
	897.11	9.975	902.61	712.664	890 $\pm$ 10 <sup>b</sup> , 886 <sup>k</sup>
	899.71	438.296	925.14	18.842	
	1287.51	0.0593	1284.96	0.3371	1285 $\pm$ 20 <sup>k</sup> , 1275 <sup>b</sup>
	2225.48	713.448	2179.37	1290.062	2104.7 <sup>b</sup> , 2097 <sup>k</sup>
	3596.90	143.912	3564.13	269.387	
	3599.41	26.106	3569.93	52.647	
C <sub>3</sub> NH	180.31	3.324	154.87	207.6288	
	190.52	1.491	187.05	38.291	
	463.33	409.108	188.75	2.815	
	592.72	2.186	563.39	8.437	
	596.46	62.223	572.20	2.130	-
	965.33	0.683	953.06	23.805	
	1957.85	27.241	2028.00	259.828	
	2293.10	1589.606	2309.68	2393.2106	
	3718.05	448.645	3760.19	1561.688	
<sup>b</sup> Birk and Winnewisser, 1986					
<sup>k</sup> King and Strope, 1971					

Table 4: Electronic transitions of precursors HNCNH and C<sub>3</sub>NH of adenine at B3LYP/6-311++g(d,p) level theory in gas phase and H<sub>2</sub>O ice containing grain phase

Species	Wavelength (gas phase) (in nm)	Absorbance	Oscillator strength	Transitions	Wave length (H <sub>2</sub> O ice) (in nm)	Absorbance	Oscillator strength	Transitions
C <sub>3</sub> NH	182.6	47462.573	0.9608	1-A'→1-A'	191.57	61654.567	1.5193	1-A→1-A
	126.7	12259.477	0.0073	1-A'→1-A''	143.78	10621.323	0.0276	1-A→1-A
	104.04	9869.950	0.0216	1-A'→1-A'	119.07	11042.926	0.0593	1-A→1-A
	-	-	-	-	104.3	7174.6216	0.0034	1-A→1-A
HNCNH	219.55	672.854	0.0166	1-A1→1-B2	215.94	716.869	0.0177	1-A1→1-B2
	184.83	1043.151	0.0217	1-A1→1-B1	159.3	17358.816	0.4126	1-A1→1-B2
	156.97	10575.579	0.2225	1-A1→1-B2	144.73	22602.596	0	1-A1→1-A2
	141.48	22671.816	0.4362	1-A1→1-B2	123.29	8869.585	0.1003	1-A1→1-A1
	102	18576.3854	0	1-A1→1-A2	100.94	14075.884	0.0338	1-A1→1-B2
	-	-	-	-	87.24	5237.201	0.1028	1-A1→1-B1

Table 5: Theoretical rotational parameters of adenine and its two precursors HNCNH and C<sub>3</sub>NH at B3LYP/cc-pVTZ level of theory

Species	Rotational constants	Values in MHz	Distortional constants	Values in MHz
HNCNH in gas phase	A	378941.67576	$D_J$	$0.30806 \times 10^{-2}$
	B	10550.84447	$D_{JK}$	$0.36739 \times 10^0$
	C	10334.08855	$D_K$	$0.11423 \times 10^3$
			$d_1$	$-0.89721 \times 10^{-5}$
			$d_2$	$-0.12535 \times 10^{-4}$
C <sub>3</sub> NH in gas phase	A	1431947.28270	$D_J$	$0.48833 \times 10^{-3}$
	B	4694.90368	$D_{JK}$	$-0.19558 \times 10^0$
	C	4680.33880	$D_K$	$0.41486 \times 10^5$
			$d_1$	$-0.20704 \times 10^{-5}$
			$d_2$	$0.29323 \times 10^{-6}$
C <sub>5</sub> H <sub>5</sub> N <sub>5</sub> in gas phase	A	2387.05922	$D_J$	$0.19731 \times 10^{-4}$
	B	1575.31931	$D_{JK}$	$0.14017 \times 10^{-3}$
	C	949.02096	$D_K$	$0.10519 \times 10^{-4}$
			$d_1$	$-0.10350 \times 10^{-4}$
			$d_2$	$-0.49530 \times 10^{-5}$

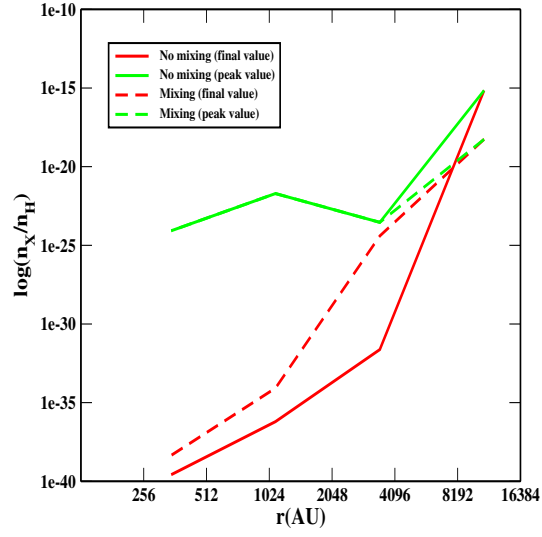


Fig. 3.— Radial distribution of adenine when mixing and no mixing models are considered. Due to heavy mixing the final and peak abundances (dashed lines) become similar.

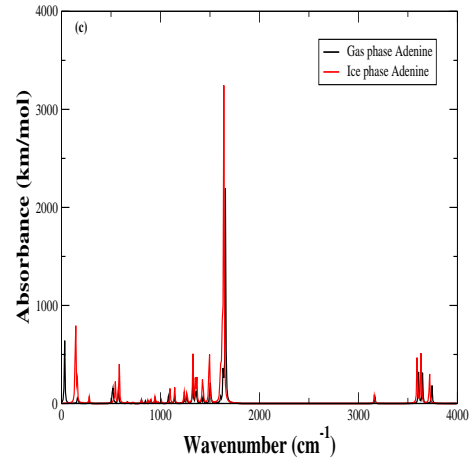
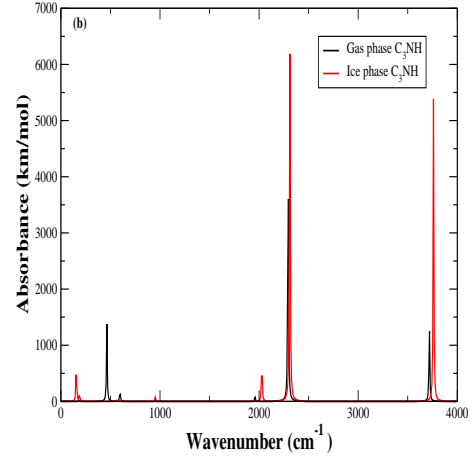
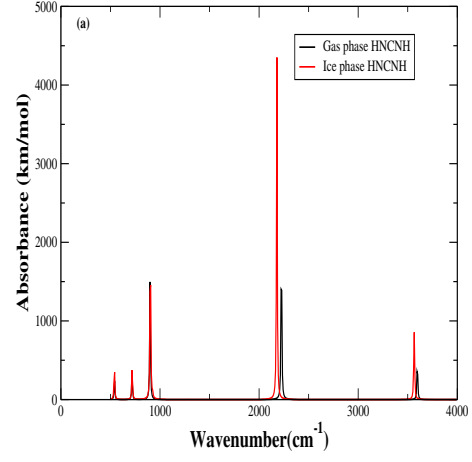


Fig. 4.— Infrared spectra of HNCNH, C<sub>3</sub>NH and adenine in gas and grain (water ice) phases.

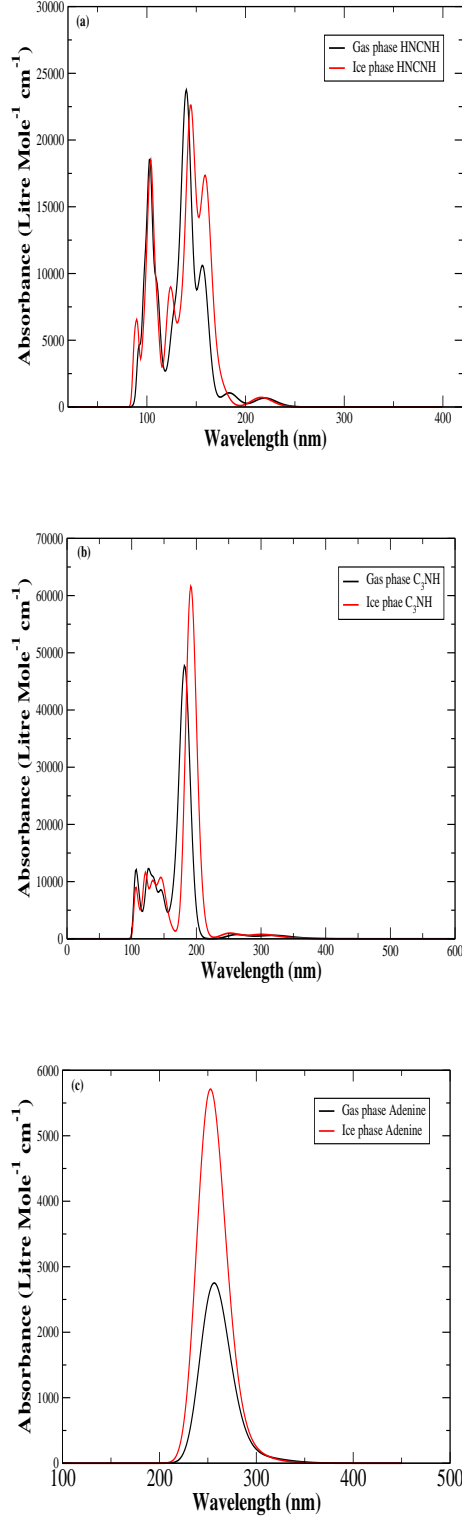


Fig. 5.— Electronic absorption spectra of HNCNH, C<sub>3</sub>NH and adenine in gas and grain (water ice) phases.

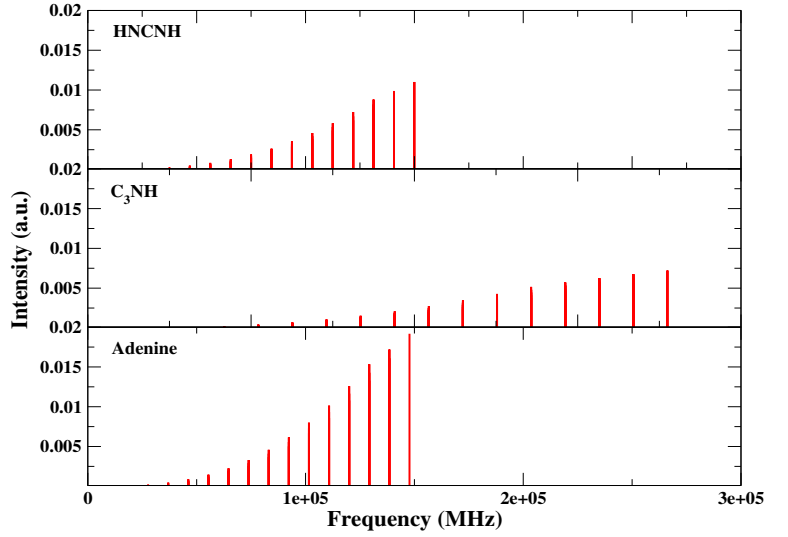


Fig. 6.— Rotational stick diagrams of HNCNH, C<sub>3</sub>NH and adenine.

## REFERENCES

- Abelson, P. H. 1966, *Proc. Natl. Acad. Sci.*, 55, 1365
- Bale, C.D., McCarthy, M.C., & Thaddins, P., 2000, *APJ*, 528, L61
- Bates, D.R, *APJ*, 270, 564
- Birk, M., Winnewisser, M., 1986, *Chem. Phys. Lett.*, 123, 5, 386
- Blagojevic, V., Petrie, S., & Bohme, D. K., 2003, *MNRAS*, L7
- Boogert, A.C.A & Ehrenfreund, P., 2004, *ASPC* 309, 547
- Brunken, S., McCarthy, M. C., Thaddeus, P., Godfrey, P. D., Brown, R. D., 2006, *A&A*, 459, 317
- Carles, S., Mollendal, H., and Guillemin, J. C., 2013, *A&A*, 558, A6
- Chakrabarti, S. & Chakrabarti, S.K., 2000a, *A&A*, 354, L6
- Chakrabarti, S.K. & Chakrabarti, S, 2000b, *Ind. J. Phys*, 74B, 97
- Chakrabarti S. K., Das, A., Acharyya, K. & Chakrabarti, S. K., 2006a, *A&A*, 457, 167
- Chakrabarti S. K., Das, A., Acharyya, K. & Chakrabarti, S. K., 2006b, *BASI*, 34, 299
- Cherchneff, I, Glassgold, A. E., Mamon, G. A., 1993, *APJ*, 410, 188
- Cuppen, H. M. & Herbst, E., 2007, *APJ*, 668, 294
- Das, A., Chakrabarti, S. K., Acharyya K. & Chakrabarti, S., 2008a, *NEWA*, 13, 457
- Das, A., Acharyya, K., Chakrabarti, S. & Chakrabarti, S. K., 2008b, *A & A*, 486, 209
- Das, A., Acharyya, K. & Chakrabarti, S. K., 2010, *MNRAS* 409, 789
- Das, A. & Chakrabarti, S. K., 2011, 418. 545, *MNRAS*
- Das, A., Majumdar, L., Chakrabarti, S. K., & Chakrabarti S., 2013a, *NEWA*, 23, 118
- Das, A., Majumdar, L., Chakrabarti, S. K., & Saha, R., Chakrabarti, S., 2013b, *MNRAS*, 433, 3152
- Das, A., Majumdar, L., Chakrabarti, S. K., & Sahu, D., 2015, *NEWA*, 35, 53
- Fuente, A., Garcia-Burillo, S. & Gerin, M., et al. 2005, *ApJ*, 619, L155
- Garrod, R.T., Wakelam, V., Herbst, E., 2007. *A&A* 467, 1103
- Gibb, E. L., Whittet, D. C. B., Boogert, A. C. A., Tielens, A. G. G. M., 2004, *ApJS* 151,35
- Guelin, M., & Cernicharo, J., 1991, *A&A*, 244, L21
- Guelin, M., Brouillet, N., Cernicharo, J., Combes, F. & Wootten, A. 2008, *Ap&SS*, 313, 45G
- Gupta, V.R, Tandon, P., Rawat, P., Singh, R.N. & Singh, A., 2011, *A&A*, 528, A129
- Hasegawa T., Herbst E., 1993, *MNRAS*, 261, 83
- Hasegawa, T.I, Herbst, E., Leung, C.M., 1992, *APJ*, 82, 167
- Herbst, E., & Woon, D.E., 1997, *ApJ*, 489, 109
- Hudson R. L., & Moore, M. H. 2004, *ICARUS*, 172, 466
- Ioppolo, S., Cuppen, H. M., Romanzin, C., Van Dishoeck, E. F., Linnartz, H., 2008, *APJ*, 686, 1474
- Jalbout, A. F., Shipar, M. A. H., 2008, *J. Chem. Sci.*, 120, 329
- Jiurys, L. M. 2006, *Proc. Nat. Acad. Sci.*, 103, 12274
- King, S.T. & Strope, J.H., 1971, *J. Chem. Phys.*, 54, 3, 1289.
- Kisiel, Z., Biakowska-Jaworska, E., Pszczkowski, L., 1998, *J. Chem. Phys.*, 109, 10263
- Kisiel, Z., Biakowska-Jaworska, E., Pszczkowski, L., *J.Mol.Spectrosc.*, 2000, 199, 5
- Liszt, H., Lucas, R. 2001, *A&A*, 370, 1
- Majumdar, L., Das, A., Chakrabarti, S.K., Chakrabarti, S., 2013, *New Astronomy*, 20, 15
- Majumdar, L., Das, A., Chakrabarti, S.K., Chakrabarti, S., 2012, *Research in Astronomy & Astrophysics*, 12, 1613
- Majumdar, L., Das, A., Chakrabarti, S.K., 2014a, *ApJ*, 782, 73
- Majumdar, L., Das, A., Chakrabarti, S.K., 2014, *A&A*, 562, A56
- McKellar, A. 1940, *PASP*, 52, 187
- McGonagale, D., Irvine, W.M., 1996. *A&A* 310, 970.
- McGuire, B., Loomis, R. A., Charness, C., Corby, J. F. et al., 2013, *AAS*, 22135209
- Merz, K. M., Aguiar, E. C., Silva, J. B. P. d, 2014, *JPhCA*, DOI: 10.1021/jp5018778
- Millar, S.L., 1953, *Science*, 117, 528
- Muller, H. S. P., Schloder, F., Stutzki, J., Winnewisser, G., 2005, *JMoSt*, 742, 215
- Muller, H. S. P., Thorwirth, S., Roth, D. A., Winnewisser, G., 2001, *A&A*, 370, L49
- Oberg, K. I., Garrord, R. T., Van Dishoeck E. F., Linnartz, H., 2009, *A&A* 504, 891
- Orgel, L. E. 2004, *Biochem Mol. Biol.*, 39, 99
- Pieve, F. Da, Avendano-Franco, G., Proft, F. De, Geerlings, P., 2014, *MNRAS*, 440,494
- Park, S-W, Lee, S, *Bull. Korean Chem. Soc.*, 2002, Vol.23, No.11
- Pickett, H. M., *J. Mol. Spectrosc.*, 1991, 148, 371
- Puletti F., Mallocci G., Mulas G., Cecchi-Pestellini C., 2010, *MNRAS*, 402,1667
- Runge, E., Gross, E. K. U., 1984, *Phys. Rev. Lett.*, 52, 997
- Rubalcava, Hector, 1956, Ph.D. thesis, California Institute of Technology. <http://resolver.caltech.edu/CaltechETD:etd-06242004-155629>
- Sahu, D., Das, A., Majumdar, L., Chakrabarti, S. K., 2015, *NewA* (in press)

- Sivaraman, B., Narayanan, R., Das, A., Gopakumar, G., Majumdar, L., Chakrabarti, S. K., Subramanian, K. P., Raja Sekhar, B. N., Hada, M., 2014, MNRAS (in press), 2014arXiv1412.5582S
- Shu, F.H., 1977, ApJ, 214, 488
- Smith, I.W.M, Talbi, & Herbst, E., 2001, A&A, 369, 611
- Snyder, L. E., & Buhl, D. 1971, ApJ, 163, L47
- Sorrell, W. H. 2001, ApJ, 555, L129
- Turner, V. E., List, H. S., Kaifu, N., & Kisliakov, A. G. 1975, ApJ, 201, L149
- Woodall, J., Agn dez, M., Markwick-Kemper, A. J., & Millar, T. J. 2006, A&A, 466, 1197
- Woon, D.E. 2002, ApJ.571, L177